Optical Properties of the Donor Tin in Gallium Phosphide

P. J. Dean, R. A. Faulkner, and S. Kimura*

Bell Telephone Laboratories, Murray Hill, New Jersey 07974

(Received 13 July 1970)

The donor Sn substitutes for Ga in GaP. Electrons bound to Ga-site donors have a pseudo-p-state representation, in contrast to P-site donors which have simple s-like ground states. We report the first optical study of such a substitutional donor in a semiconductor. Analysis of the weak no-phonon structure in donor-acceptor-pair luminescence spectra, characteristic of Ga-site donors, indicates that $(E_D)_{Sn} = 65.5 \pm 1$ meV. Central-cell enhancement of E_D is expected to be small for donors with p-like ground states, and Sn is by far the shallowest donor so far identified in GaP. We have seen absorption and luminescence of excitons bound to the neutral Sn donor. The exciton localization energy is ~ 10 meV, lower than that observed for excitons bound to the deeper P-site donors S, Se, and Te, in rough accord with Haynes's rule. Magneto-optical studies of the principal (lowest-energy) no-phonon component in the Sn exciton luminescence spectrum show that the initial state contains a single unpaired hole, and the final state contains a single unpaired electron with a small negative g factor. The ground state of the Sn donor can be split into a $p_{3/2}$ state (Γ_8) and a $p_{1/2}$ state (Γ_7) by spin-orbit interaction. The sign and magnitude of the electron g factor indicates that the $p_{1/2}$ state lies lowest for the Sn donor. The g factor for the "orbital" part of the wave function of the Sn donor p state is essentially zero, as expected for a "valley-orbit" p state. This identification is confirmed by the observation that the ground state of the Sn donor is not split by uniaxial stress for any crystallographic orientation of the stress. The magnitude of the $\Gamma_7 \rightarrow \Gamma_8$ splitting of the Sn donor ground state is 2.1 ± 0.1 meV, determined roughly from an analysis of nonlinear shifts in the Zeeman pattern of the Sn exciton, and more precisely from the energies of weak "two-electron" transitions in which the donor is left in the Γ_8 state, observed in the zero-field spectra. The decay time from the lowest state of the Sn exciton is 90 nsec, some 2700 times shorter than that determined from the experimental absorption cross section of this transition. This large discrepancy is attributed to the predominance of nonradiative (Auger) recombinations of the Sn exciton.

I. INTRODUCTION

The optical properties of shallow P-site donors in GaP have been extensively studied.[1,2] These donors induce near-band-gap donor-acceptor-pair and bound-exciton transitions with relatively large oscillator strength, even though GaP is an indirect semiconductor. The strength of these optical transitions derives from the fact that the lowest conduction-band minima, at $\langle 100 \rangle$-type symmetry points, have X_1 symmetry according to a representation based upon donor ions on the electron-attractive (P) sublattice.[3] Thus, the Bloch part of the wave function of an electron trapped at a shallow P-site donor has an antinode at the donor core. Given suitable intermediate conduction-band states, the central-cell interaction of the electron at the donor core can then produce no-phonon and phonon-assisted recombinations with significant transition probabilities.[3]

The intermediate state favored by the form of the GaP band structure is $(\Gamma_1)_c$. Morgan[3] has shown that for an attractive donor-core interaction, the donor ground state is $1s(A_1)$ and no-phonon recombination with a band-edge hole can take place through the $(\Gamma_1)_c$ state. In addition, phonon-assisted recombinations involving only LA momentum-conserving (MC) phonons are allowed via the $(\Gamma_1)_c$ interme-

diate state. On the other hand, donors on the Ga lattice site have a lowest-energy state transforming as $1s(T_2)$ with a node in the electron wave function at the donor core. No-phonon recombinations involving this electron are allowed by symmetry only via energetically unfavorable intermediate conduction-band states well above $(\Gamma_1)_c$, although LA phonon-assisted transitions via $(\Gamma_1)_c$ are still allowed.

The large differences in oscillator strength for no-phonon transitions involving the Ga-site donor Si and P-site donors such as S have been demonstrated experimentally through a study of electron-hole recombinations at donor-acceptor pairs.[4,5] In this paper, we extend these observations to the Ga-site donor Sn, which is significantly shallower than Si and induces even weaker no-phonon-pair transitions. We obtain an accurate estimate of the ionization energy of the Sn donor from these spectra (Sec. III A). We have also observed the absorption and luminescence of excitons weakly bound to the shallow Sn donor. The relative strengths of the no-phonon transition and the different MC phonon replicas (Sec. III B) are consistent with expectation from the spectra of excitons bound to P-site donors[2] and from recently discovered spectra of excitons bound to shallow acceptors in GaP.[6] The lowest Sn exciton no-phonon line splits in a magnetic field (Sec. III C) and under uniaxial stress (Sec. III D) as

expected if the large degeneracy possible for the wave function of a Ga-site donor in GaP has been partially lifted by a "valley-orbit" quasi-spin-orbit interaction. There is a substantial quenching of the g value of electrons bound to the Sn donor. The spin-orbit splitting of the donor ground state is 2.1 meV, according to the displacement below the principal Sn exciton lines of satellite lines due to "two-electron" transitions in which the donor is left in the spin-orbit excited state. This value is consistent with a rough estimate obtained from nonlinear terms in the Zeeman splitting of the principal exciton transition. The weak optical absorption attributed to Sn bound excitons (Sec. III E) indicates a radiative decay time ~2700 times longer than the observed exponential decay time of ~90 nsec. This discrepancy is attributed to a predominantly nonradiative (Auger) decay of excitons bound to the neutral Sn donor, as previously observed[6] for generically similar bound exciton transitions in indirect-gap semiconductors like GaP.

II. EXPERIMENTAL

A. Crystal Growth

The reduced oscillator strength of transitions induced by Ga-site donors places stringent requirements on the quality of crystals in which these transitions are to be studied. Most of our Sn-doped single crystals were prepared either from Ga solution or by vapor growth with wet hydrogen transport, using the open-tube furnace system described elsewhere.[4] Tin was added from a metallic source placed typically at ~1000 °C upstream of the alumina boat loaded with Ga. Concentrations of optically active N and S in the vapor-grown needles were typically $\lesssim 10^{14}$ cm^{-3} and $\lesssim 10^{15}$ cm^{-3}, the respective sensitivity limits of the analysis technique using the bound-exciton absorption induced by these P-site impurities with needles ~0.5 cm long. Zinc-Sn double-doped needles were prepared by adding a source of metallic Zn at ~450 °C upstream of the Ga boat. Some halide-transport epitaxially grown Sn-doped GaP crystals, grown by Luther, were particularly suitable for the uniaxial stress studies. Carbon-Sn pair spectra were observed from crystals grown by Verleur using the liquid encapsulated Czochralski technique.[7] In this case, metallic Sn was simply added to the GaP charge from which the single crystal was pulled.

B. Optical Measurements

Luminescence spectra of the Sn exciton were recorded photographically on a 2-m $f/17$ Bausch and Lomb spectrograph using freely suspended crystals immersed in liquid He pumped below the λ point. The luminescence was excited by 4880-Å radiation from an Ar$^+$ laser. The decay time of the lumines-

cence was measured in a straightforward manner using a Tektronix 1S1 sampling scope or a PAR model 160 boxcar integrator to display the luminescence response to excitation by pulses of 4880-Å light of half-width ~10 nsec obtained with an acousto-optical intracavity laser modulator.[8] Structured donor-acceptor-pair spectra were also recorded photographically. Zeeman spectra were obtained using either a 12-in. Varian electromagnet with the Bausch and Lomb spectrograph, or a Westinghouse superconducting magnet with a 1-m Jarrell-Ash spectrograph. Spectra of unresolved transitions at very distant donor-acceptor pairs were obtained photoelectrically with a $\frac{3}{4}$-m $f/6.8$ Spex 1401 scanning monochromator, using minimal excitation of unfocussed penetrating 5145-Å light from an Ar$^+$ laser.

III. RESULTS AND DISCUSSION

A. Donor-Acceptor-Pair Spectra

Luminescence spectra recorded under very low photoexcitation intensity from three double-doped GaP crystals are shown in Fig. 1. It is clear that the three spectra all have the general form origi-
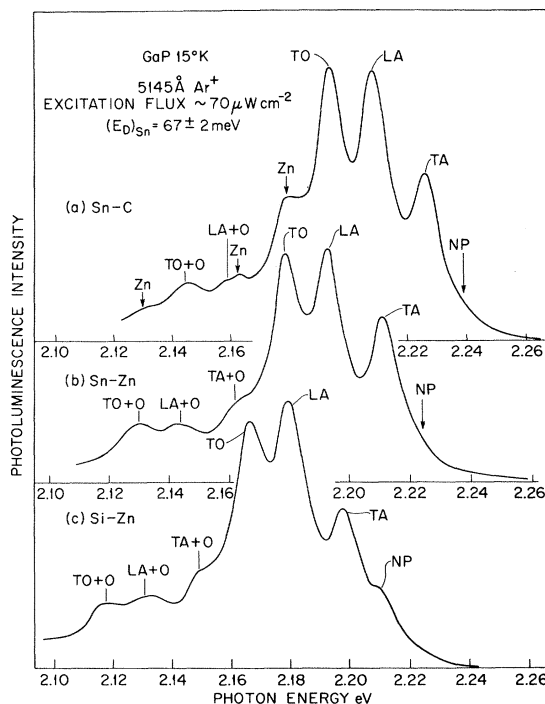

FIG. 1. Low-temperature photoluminescence of GaP involving electron-hole recombinations at pairs of the donors Sn and Si and the acceptors C and Zn, as indicated, recorded under very low-level excitation. The Sn-C pair spectrum in (a) is slightly contaminated by Sn-Zn, as shown. The spectra are dominated by replicas of the very weak no-phonon (NP) distant pair peaks due to transitions involving the emission of TA, LA, and TO MC phonons.

nally reported for pair transitions involving the Si donor,[4,5] in which the principal components are due to TA, LA, and TO momentum-conserving phonon-assisted recombinations. The shifts in the peak energies of these components reflect differences in the ionization energies of the acceptors Zn and C or of the donors Si and Sn. The energy difference

$$(E_A)_{Zn} - (E_A)_C = 15.5 \text{ meV}$$

according to spectra (a) and (b) in Fig. 1, in good agreement with previous estimates.[4] The energy displacement between corresponding components in spectra (b) and (c), allowing for the slight increase in the saturation of spectrum (c), suggests that[9]

$$(E_D)_{Si} - (E_D)_{Sn} \sim 14.5 \text{ meV},$$

i.e.,

$$(E_D)_{Sn} = 68 \text{ meV if } (E_D)_{Si} = 82.5 \text{ meV} .$$

Replicas of the principal components occur at lower energies due to the simultaneous emission of ~ 49-meV optical phonons (0).

The distant pair peak due to no-phonon recombinations in these pair spectra is very weak,[5] but can

be clearly seen in the Si-Zn spectrum in Fig. 1. Relative to the principal components due to phonon-assisted transitions, the no-phonon components in the Sn-C and Sn-Zn pair spectra are substantially weaker than in the Si-Zn spectrum. The principal components are slightly better resolved in the Sn-C and Sn-Zn pair spectra than in the Si-Zn spectrum, so the difference in visibility of the no-phonon transition is not an artifact of spectral broadening. This difference between the pair spectra involving Si and Sn donors demonstrates that a large fraction of the oscillator strength for no-phonon transitions is due to the donor-electron interaction, even for Ga-site donors in GaP. Such behavior is consistent with the surprising fact that the central-cell correction almost doubles the ionization energy of the Si donor, in spite of the symmetry arguments for Ga-site donors mentioned above. This enhancement may be due to dielectric breakdown at short range *around* the donor core.

It was just possible to observe the low oscillator strength no-phonon transitions at discrete Sn-Zn donor-acceptor pairs (Fig. 2). The individual
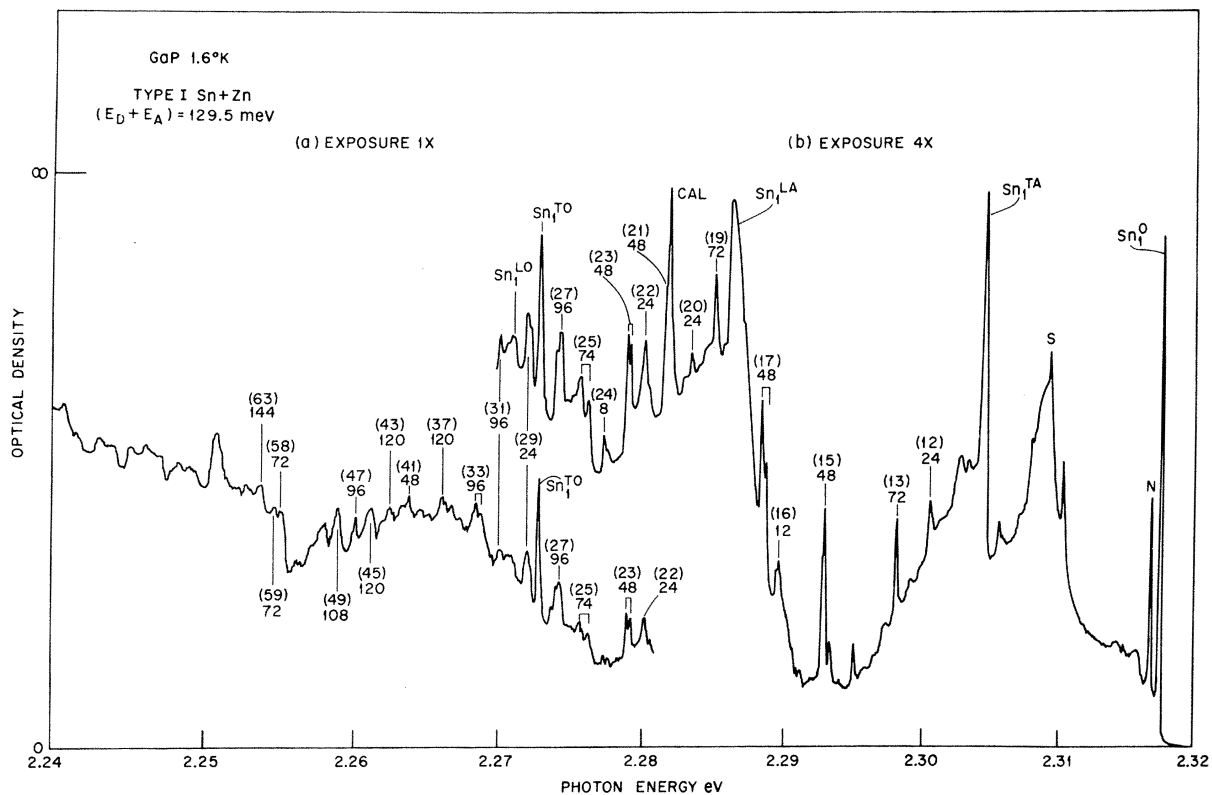

Fig. 2. Section of the low-temperature spectrum of GaP, recorded photographically, showing no-phonon transitions at discrete Sn-donor–Zn-acceptor pairs. The bracketed numbers are the shell numbers, an index of the distances to Sn donors from a given Zn acceptor allowed in the GaP lattice. The remaining numbers are the numbers of equivalent pairs within each shell. Lines N and S are due to the no-phonon recombination of excitons bound to N isoelectronic traps and to neutral S donors.

lines arise from transitions at pairs with differing lattice separation, since the transition energy $h\nu$ depends on the pair separation r according to[10]

$$h\nu = E_g - (E_A + E_D) + \frac{e^2}{\epsilon r} - \left(\frac{e^2}{\epsilon r}\right)\left(\frac{b}{r}\right)^5 \quad , \qquad (1)$$

where ϵ is the low-temperature static dielectric constant, 10.75 in GaP,[11] E_A and E_D are the ionization energies of the donor and acceptor, E_g is the energy gap, e is the electronic charge, and b is a constant for a given donor-acceptor pair. For $r \gg a_0$, the ground-state radius of the least polarizable neutral center,[12,13] the fourth term in Eq. (1) can be identified with the van der Waals polarization interaction between the neutral donor and acceptor, whereupon $b = (6.5)^{1/5} a_0$.[13]

The assignments of a shell number to the lines in Fig. 2 were made in the usual way.[4,10] The Sn-Zn pair spectrum is type I, that is, both impurities are on Ga lattice sites. The fine structure expected within the set of transitons for a given shell, containing pairs of given r, arising from the several different subsets of crystallographically inequivalent pairs which occur for most values of r, are not well resolved in this spectrum. These splittings are small for very shallow impurities, as shown by a comparison of S-C and Te-C pair spectra in GaP. Such substructure as is resolved in Fig. 2, and the relative strengths of adjacent lines, including the gap in the spectrum for $m = 14$ near 2.295 eV, are in satisfactory agreement with the assignments given in Fig. 2. The fit of Eq. (1) to the transition energies is shown in Fig. 3. For $r \gtrsim 23$ Å, only the first three terms need be considered, as has been found for other shallow-pair spectra in GaP.[10,14] The van der Waals term would improve the fit over a limited range of r, perhaps down to 18 Å. For smaller r, the pair separation is smaller than the sum of the ground-state radii of the donor and acceptor, and the dielectric continuum expression in Eq. (1) becomes inapplicable.

The fit in Fig. 3 neglecting the van der Waals term provides an accurate estimate of $(E_A + E_D)$, the only adjustable parameter. We find

$$(E_A + E_D) = 129.5 \pm 1 \text{ meV, if } E_g = 2.339 \pm 0.001 \text{ eV.}$$

Since $(E_A)_{Zn} = 64 \pm 1$ meV, we conclude that $(E_D)_{Sn} = 65.5 \pm 1$ meV, consistent with the less accurate estimate obtained from Fig. 1. This is the shallowest donor known in GaP. Hall-effect studies on these Sn-doped crystals[15] yield thermal activation energies of 56 meV for $N_D = N_A = 5.3 \times 10^{17}$ cm^{-3}. Measurements of the concentration dependence of shallow Te donors[16] and Zn acceptors[17] in GaP suggests that a concentration-induced reduction of ~10 meV in the thermal value of $(E_D)_{Sn}$ is reasonable at this concentration level.
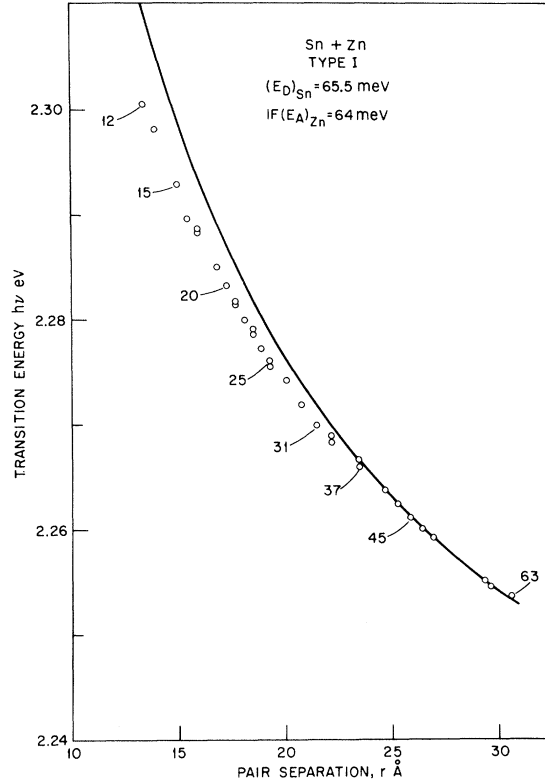

FIG. 3. Transition energy of recombinations at discrete pairs of Sn donors and Zn acceptors in GaP as a function of the pair separation. The curve is the best fit of Eq. (1), neglecting the van der Waals polarization interaction term. Some shell numbers are indicated.

B. Luminescence of Excitons Bound to Neutral Tin Donors

A new series of sharp lines and associated replicas appears in the near-band-gap low-temperature photoluminescence spectrum of lightly Sn-doped GaP (Fig. 4). Comparison with the luminescence of other donor- and acceptor-exciton complexes[2,18] in GaP suggests the assignments given. At the lowest temperatures (excitation levels) only the lowest no-phonon line Sn_1^0 is seen. This line is only 10 meV below the exciton energy gap E_{gx} so the exciton must be bound to the *neutral* Sn donor.[19] Component Sn_1^0 is replicated by strong X components associated with the emission of TA, LA, and TO phonons, whose energies are consistent with values obtained from Fig. 1 and also from other shallow bound-exciton spectra in GaP (Table I). These components are strong because they represent transitions in which the crystal momentum selection rule for indirect transitions is satisfied by coupling to phonons whose wave-vector matches the wave-vector difference between electrons at the conduction-band minima and holes at the valence-band maxima. We shall call these MC phonons. The assignments have been made by fitting the energies

TABLE I. Energies of MC phonons derived from the luminescence of excitons bound to neutral donors and acceptors in GaP.

Impurity	$\hbar\omega_{TA}$[a] (meV)	$\hbar\omega_{LA}$[a] (meV)	$\hbar\omega_{TO}$[a] (meV)	$\hbar\omega_{LO}$[a] (meV)
S (D)	13.1	31.4	45.2	?
S (D)	13.2	31.6	45.3	?
Te (D)	13.1	31.5	45.3	46.8
Sn (D)	13.2	31.7	45.4	46.7[b]
C (A)	13.1	31.7	45.5	
Mg (A)	13.1	31.6	45.5	
Zn (A)	13.2	31.7	45.4	46.8
Cd (A)	13.1	31.8	45.4	46.9

[a]Experimental error ±0.1 meV.

[b]Partially obscured by $Sn_{2,X}^{TO}$ except at lowest temperatures (Figs. 4 and 5).

in Table I to the phonon dispersion curves of GaP.[20] This fit confirms that the conduction-band minima must lie at or very close to the X points in the reduced zone if the valence-band maxima are at the zone center (Γ).

The relatively weak replica due to the emission of MC LO phonons (Table I) is also visible in Fig. 4. This replica has also been seen in the luminescence of excitons bound to shallow acceptors in GaP.[18] It was not recognized in the luminescence of excitons bound to P-site donors because of masking by prominent replicas involving optical phonons not selected by momentum conservation.[2]

Table II shows that the relative intensities of the Sn donor and Cd acceptor no-phonon lines are comparable. This is a reasonable result, since the

exciton localization energies $E_{BX} = E_{gx} - h\nu^0$ are comparable for Sn and Cd and the electron wave function is excluded from the impurity core for both of these exciton complexes. Here $h\nu^0$ is the recombination energy of the bound exciton. Pursuing the arguments presented in Sec. I, the fractional oscillator strength in the Sn exciton no-phonon line should be given by

$$(f_0)_{Sn,Cd} = \frac{1}{21}[(E_{D,A})_{Sn,Cd}/(E_D)_S]^{5/2}(f_0)_S , \qquad (2)$$

where the factor of $\frac{1}{21}$ is the approximate ratio of the squared energy denominators for electron scattering via the energetically favored $(\Gamma_1)_C$ intermediate state in GaP compared with electron scattering via higher conduction-band states or hole scattering through the most favorable valence-band intermediate states.[21] The values of $(f_0)_{Sn,Cd}$ calculated using Eq. (2) give intensity ratios of phonon-assisted to no-phonon transitions significantly smaller than experiment. The values of (f_0) vary widely between the P-site donors S, Se, and Te, however.[2] Using the observed value of $(f_0)_{Se}$, Eq. (2) gives fair agreement with experiment for $(f_0)_{Te,Sn,Cd}$, but the calculated values of f_0 are still much larger than experiment for the shallower acceptors C, Mg, and Zn (Table II). Table II also shows that the relative strengths of MC phonon replicas are nearly constant for excitons bound to Ga and P-site donors and acceptors, as expected from Sec. I, except that the LA replicas are exceptionally strong for the very shallow acceptors C and Mg.

The weak components below 2.27 eV in Fig. 4

TABLE II. Parameters of absorption and luminescence of excitons bound to some neutral donors and acceptors in GaP. The I_S are integrated intensities for the no-phonon (subscript 0) and MC phonon replicas, measured in luminescence (L) and absorption (A).

Impurity	Ionization energy (meV)	I_{TA}/I_0	I_{LA}/I	I_{TO}/I_0	$(I_{LA}/I_0)_{calc}$[a]	$(I_{LA}/I_0)_{calc}$[b]
Sulphur (D)	104.0	0.009 (L) 0.011 (A)	0.015 (L) 0.02 (A)	0.005 (L) ~0.005 (A)		0.080 (L, A)
Selenium (D)	102.0	0.050 (L) 0.053 (A)	0.084 (L) 0.083 (A)	0.03 (L)	0.016 (L) 0.021 (A)	
Tellurium (D)	89.5	0.021 (L) 0.02 (A)	0.13 (L) 0.03 (A)	0.005 (L)	0.022 (L) 0.029 (A)	0.12 (L, A)
Tin (D)	65.5	2.3 (L)	5.5 (L)	1.1 (L)	1.0 (L) 1.3 (A)	5.3 (L, A)
Carbon (A)	48.0	54 (L)	250 (L)	25 (L)	2.2 (L) 2.9 (A)	12 (L, A)
Magnesium (A)	53.5	13 (L)	40 (L)	~5 (L)	1.7 (L) 2.2 (A)	8.8 (L, A)
Zinc (A)	64.0	22 (L) 266 (A)	54 (L) 88 (A)	12 (L)	1.1 (L) 1.4 (A)	5.6 (L, A)
Cadmium (A)	96.5	1.1 (L) 2.2 (A)	1.8 (L) 4.7 (A)	0.51 (L)	0.38 (L) 0.5 (A)	2.0 (L, A)

[a]Calculated using the relation $(f_0)_{A,D} = \frac{1}{21}[E_{A,D}/(E_D)_S]^{5/2}(f_0)_S$; Eq. (2) of text.

[b]Calculated using the relation $(f_0)_{A,D} = \frac{1}{21}[E_{A,D}/(E_D)_{Se}]^{5/2}(f_0)_{Se}$. (The prefactor $\frac{1}{21}$ is omitted in the intercomparison of excitons bound to P-site donors.)
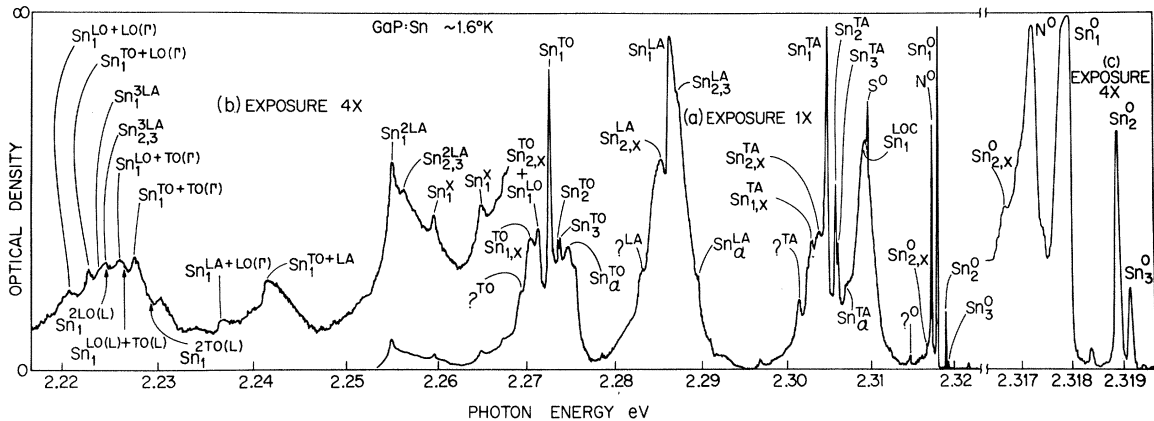
FIG. 4. Low-temperature photoluminescence of excitons bound to neutral Sn donors in GaP, recorded photographically. The no-phonon $Sn^0_{1,2,3}$ have strong replicas due to transitions in which MC phonons are emitted. Some two and three phonon-assisted transitions can be identified. Components Sn^X_1 involve "two-electron" transitions which leave the Sn donor in orbital excited states, while $Sn_{1,X}$ and $Sn_{2,X}$ are "two-electron" transitions which leave the Sn donor in the upper $\Gamma_8(p_{3/2})$ component of the ground state which is split by spin-orbit interaction. Component Sn^{LOC}_1 is believed due to a phonon-assisted transition involving the emission of a local mode. The vertical arrows near 2.227 eV are discussed in the text. Part (C) contains a long exposure and an extended energy scale to show the excited states $Sn^0_{2,3}$ more clearly.

mainly arise from transition Sn^0_1 occurring with the emission of two or more phonons. In fact they are mostly phonon replicas of the strong components Sn^{LA}_1 and Sn^{TO}. Momentum conservation is already assured by the phonon interaction for the latter components. The additional phonons are either those of zero wave vector [TO(Γ) and LO(Γ)] or else there is a second interaction with the ~ 31.5-meV LA phonon at X, presumably resulting in electron scattering between conduction-band valleys on different $\langle 100 \rangle$-type axes (f scattering[22]) during the recombination process. Similar multiphonon-assisted recombinations have been observed for excitons bound to neutral acceptors.[18] In neither case have multiple-phonon-assisted transitions involving L ($\langle 111 \rangle$ zone boundary) phonons been observed (see the arrows between 2.22 and 2.23 eV in Fig. 4). These phonon-assisted transitions are possible since

$$\tfrac{1}{2}(1, 1, 1) + \tfrac{1}{2}(1, -1, -1) = (1, 0, 0) \ , \tag{3}$$

and electron momentum is thereby conserved.

Multiple-phonon-assisted transitions obeying Eq. (3) have been claimed in β SiC,[23] which has the same type of limiting interband transitions as GaP.

The broad component Sn^{LOC}_1, underlying the sharp S^0 exciton line in Fig. 4, is a persistent feature of the Sn exciton luminescence spectrum. It is superscripted LOC because it is probably due to a phonon-assisted transition involving the emission of a ~ 9-meV in-band resonance local mode characteristic of Sn on Ga lattice sites. The Te bound exciton spectrum contains a broad satellite displaced 23 meV below the no-phonon line, and a similar assignment has been suggested for it.[2]

Although the bath temperature for the spectrum in Fig. 4 was 1.6 °K, the local lattice temperature was deliberately raised by intense optical excitation (85-mW focused light from Ar$^+$ laser) to reduce the thermalization factor in order to display the excited states Sn^0_2 and Sn^0_3 of the Sn exciton and their phonon replicas. It was noticed that the relative intensity of weak components just below the principal Sn_1-series components was very temperature sensitive. This is shown more clearly in the photoelectric spectra in Fig. 5, where spectrum (b) was recorded at a *sample* temperature of 1.6 °K while spectrum (a) was recorded at a bath temperature of 4.2 °K with some additional heating due to optical pumping. Components $Sn^0_{2,X}$, $Sn^{TA}_{2,X}$, and $Sn^{LA}_{2,X}$ are much stronger at ~ 5 °K than at 1.6 °K. They were found to bear a constant intensity ratio so Sn^0_2. Components $Sn^{TA}_{1,X}$, $Sn^{LA}_{1,X}$, and $Sn^{TO}_{1,X}$ are similarly related to Sn^0_1, although the intensity ratio of the associated no-phonon component and Sn^0_1 is only ~ 1% of the corresponding ratio $Sn^0_{2,X}/Sn^0_2$. The energy separation of the $Sn_{1,X}$ and $Sn_{2,X}$ series is ~ 0.9 meV, identical to that of Sn^0_1 and Sn^0_2 (0.97 meV) within experimental error. The Sn_1 series does not thermalize into $Sn_{1,X}$, neither does the Sn_2 series thermalize into $Sn_{2,X}$, even though the relevant energy separations are ~ 2.1 meV (~ 15kT at 1.6 °K). These observations suggest that this splitting is in the ground state of the transition. The observed behavior is consistent with the level diagram in Fig. 6, where the 2.1-meV ground-state splitting is attributed to the "spin-orbit" splitting of the p-like electron on the Sn donor. This excitation energy is far too small to represent transitions to orbital excited states of the Sn donor.[24] The assignments
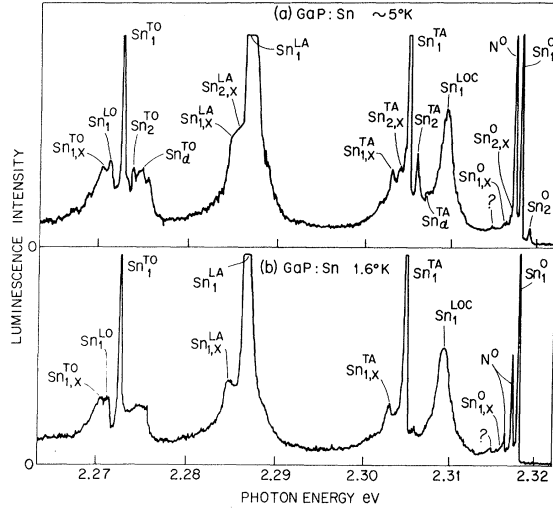
FIG. 5. Low-temperature photoluminescence of exci-
tons bound to neutral Sn donors, recorded photoelectri-
cally. Spectrum (a) recorded at 5 °K shows excited state
Sn_2^0 and its associated phonon replicas $Sn_2^{TA,LA,TO}$ and
"two-electron" transitions $Sn_2^{0,TA,LA}$. The luminescence
near Sn_1^{LO} is enhanced by $Sn_{2,X}^{TO}$ unresolved from it.
These components are absent from spectrum (b), re-
corded at 1.6 °K, because of thermalization in the exci-
ted state of the bound exciton. The replicas $Sn_{1,X}^{0,TA,LA,TO}$
of component Sn_1^0, due to two-electron transitions, are
clearly resolved at 1.6 °K.

in Fig. 6 will be discussed further in Sec. III C.

Additional weak features occur in the Sn exciton
luminescence spectrum. The series of weak com-
ponents Sn_α^{TO}, Sn_α^{LA}, and Sn_α^{TA} suggest the presence
of weak no-phonon transitions near 2.320 eV, which
will be discussed in Sec. III D. The two components
Sn_1^X near 2.26 eV are displaced below Sn_1^0 by 53.2
and 58.5 meV, i. e., by energies which are, re-
spectively, 12.3 and 7.0 meV lower than $(E_D)_{Sn}$
(Sec. III A). These latter energies are comparable
with the binding energies expected for principal
s- and p-like excited envelope states of the Sn do-
nor.[24] It is therefore probable that components Sn_1^X
represent two-electron transitions,[25] in which the
Sn donor is left in shallow excited states. The
series of components $?^0$, $?^{TA}$, $?^{LA}$ and $?^{TO}$ do not
bear a constant intensity relative to Sn_1^0. These
components therefore represent an independent
transition of unknown origin, possibly also con-
nected with Sn. The exciton localization energy of
$?^0$ is 13.4 meV.

The intensity ratios Sn_1^X/Sn_1^0 are ~1 to 2%, com-
parable to those observed for two-electron transi-
tions to $2s$ excited states of P-site donors in GaP.
The spectrum in Fig. 4, and those of excitons bound
to neutral acceptors in GaP,[18] do not contain satel-
lites of the strong components due to MC phonon-
assisted transitions which can be identified with
two-electron or two-hole transitions. Neither

were such transitions observed in the luminescence
of P-site donors in GaP. We conclude that the in-
tensity ratios $(Imp^{2s}/Imp^{1s})_{MC\ phon}$ are at least 10
to 100 times smaller than the observed ratios
$(Imp^{2s}/Imp^{1s})_0$.[26]

The weakness of two-electron transition replicas
of the MC phonon-assisted components can be quali-
tatively understood as follows. The wave function
of an exciton–neutral-donor complex may be written
$\psi(r_1, r_2, r_h)$, where r_1 and r_2 refer to the positions
of the two electrons relative to the donor ion. For
the no-phonon transition, r_2 and r_h are both zero.
For the MC replica, the only condition is that $r_2 = r_h$
before recombination, but these particles need not
be in the central cell. If $\psi(r_1, r_2, r_h)$ can be rep-
resented by a simple product wave function [Fig.
7(a)], then $\psi(r_1)$ is unaffected by the value of $r_2 = r_h$.
Then two-electron replicas of the no-phonon and
phonon-assisted transitions will be equally promi-
nent. This representation is a poor approximation
for these exciton complexes, however.[27]

Consider the representation of the shallow bound-
exciton state shown in Fig. 7(b). This representation
was emphasized by Haynes[28] in view of the fact that
E_{BX} is proportional to E_D for such exciton complexes
in Si. A similar trend holds for exciton-acceptor[18]
and exciton-donor complexes in GaP, although the
dependence is not smooth in the latter case (Fig. 8),
possibly because of the influence of higher conduc-
tion-band minima on the donor wave functions. In
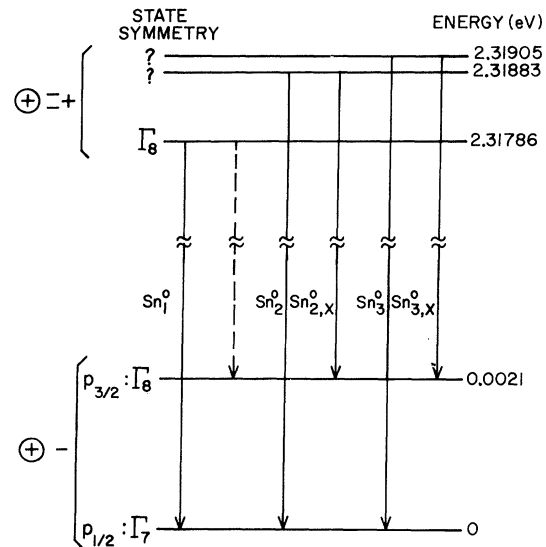Fig. 7(b), the exciton localization energy E_{BX} is

FIG. 6. Energies and symmetries of the lowest states
of excitons bound to neutral Sn donors, electrons bound
to Sn donors, and the transitions between them. The
dashed line indicates a "two-electron" transition $(Sn_{2,x})$
in which the state of the remaining electron changes from
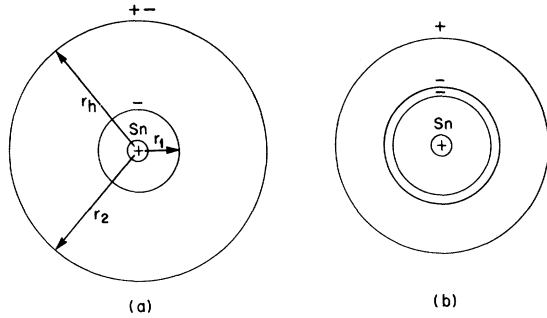Γ_7 to Γ_8 and is forbidden on the "sudden" approximation.

FIG. 7. Representations of the Sn neutral donor-exciton complex in GaP; (a) with binding due to polarization interaction, (b) with binding due to exchange interaction between the like particles (electrons).

essentially the (small) binding energy of the second electron. The electrons are indistinguishable, but the no-phonon transition involves the electron which instantaneously has more wave function in the central cell. The remaining electron will then be far from the central cell, that is, its wave function will be strongly distorted from the donor ground-state configuration and two-electron transitions will be strong. Parity will be conserved in this approximation, and the two-electron transitions will be primarily to s-like excited states, in agreement with experiment.[29] For exciton recombinations in which momentum is conserved by interaction with phonons, the configuration of the remaining electron will generally resemble the donor ground state much more closely, and the corresponding two-electron transitions will be much weaker.

C. Electronic Structure of the Bound Exciton: Zeeman Effect

The electronic structure of the ground state of a Ga-site donor such as Sn in GaP is quite different from P-site donors such as S (Sec. I). In the absence of electron spin, the Sn donor ground state is similar to a p state, transforming as Γ_5 under the T_d point group.[3] This is a "pseudo"-p-state, however. It does not split in a magnetic field; its g factor is zero.[30] The reason for this is that the (x, y, z) components of the triply degenerate Γ_5 representation represent the three valleys of the GaP conduction band and are orthogonal not only because of symmetry but also because they belong to different (inequivalent) points in the Brillouin zone. The Zeeman interaction could mix the states if they were orthogonal only by symmetry, but it cannot overcome the orthogonality due to the phase cancellation of the separate points in k space.

Inclusion of the electron spin causes a splitting of the ground state into a $p_{3/2}$ state (Γ_8) and a $p_{1/2}$ state (Γ_7) by the spin-orbit interaction (Fig. 6). The donor spin-orbit splitting should be approximately equal to the impurity atomic spin-orbit splitting

reduced by the fraction of the donor envelope wave function in the central-core region. For the Sn donor in GaP, this estimate would be in the range 2–8 meV.

In the usual treatment of spin-orbit splitting of a p state, we have the magnetic Hamiltonian ($\hbar = 1$)

$$H = \tfrac{2}{3}\Delta \vec{L} \cdot \vec{S} + \mu_B (g_L \vec{L} \cdot \vec{H} + g_S \vec{S} \cdot \vec{H}) \ , \qquad (4)$$

where Δ is the spin-orbit splitting, μ_B is the Bohr magneton, $L = 1$, $S = \tfrac{1}{2}$, g_L is the orbital g factor, g_S is the spin g factor, and H is the external magnetic field.

If $\Delta \gg g\mu_B H$, where g is either g_L or g_S, then it is appropriate to reexpress the Hamiltonian in terms of separate Hamiltonians for the $p_{1/2}$ and the $p_{3/2}$ states:

$$H_{3/2} = \tfrac{1}{3}\Delta + \mu_B (\tfrac{2}{3}g_L + \tfrac{1}{3}g_S)\vec{J} \cdot \vec{H} \ , \qquad (5a)$$

$$H_{1/2} = -\tfrac{2}{3}\Delta + \mu_B (\tfrac{4}{3}g_L - \tfrac{1}{3}g_S)\vec{J} \cdot \vec{H} \ , \qquad (5b)$$

where $\vec{J} = \vec{L} + \vec{S}$ is the total angular momentum, If $g_L \neq g_S$, there are interaction terms between the $J = \tfrac{3}{2}$ and the $J = \tfrac{1}{2}$ states.

For the pseudo-p-state we are considering $g_L \approx 0$. The Zeeman Hamiltonians for the two possible donor ground states then become

$$H_{3/2} = \tfrac{1}{3}\Delta + \tfrac{1}{3}g_e\mu_B \vec{J} \cdot \vec{H} \ , \qquad (6a)$$

$$H_{1/2} = -\tfrac{2}{3}\Delta - \tfrac{1}{3}g_e\mu_B \vec{J} \cdot \vec{H} \ , \qquad (6b)$$
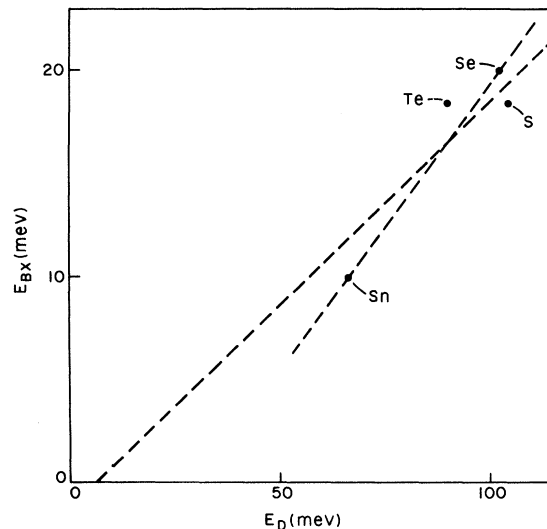

FIG. 8. Variation of the localization energy E_{BX} for excitons bound to neutral donors in GaP with the donor ionization energy. The two dashed lines indicate that the proportionality between these quantities is ill defined. One line has been drawn relatively close to the origin to follow the behavior observed for donors and acceptors in Si (Ref. 28), but not neutral acceptor-exciton complexes in GaP (Ref. 18).

where we have changed g_S to g_e, the electron spin g factor. The effective g factor of the $p_{3/2}$ state is $\frac{1}{3}g_e$ and that of the $p_{1/2}$ state is $-\frac{1}{3}g_e$, a negative quantity.

The Zeeman effect of the lowest component Sn_1^0 of the neutral Sn bound exciton is shown in Figs. 9 and 10 for magnetic fields up to 50 kG along the three principal crystallographic directions, and in Fig. 11 for a constant field of 30.5 kG rotated from [001] to [110] in the (1$\bar{1}$0) plane. The data are well represented by a model in which the initial state has a magnetic splitting characteristic of a simple weakly bound hole of angular momentum $J = \frac{3}{2}$, represented by the Zeeman Hamiltonian[31]

$$H_{init} = \mu_B[K\vec{J}\cdot\vec{H} + L(J_x^3 H_x + J_y^3 H_y + J_z^3 H_z)] \quad . \quad (7)$$
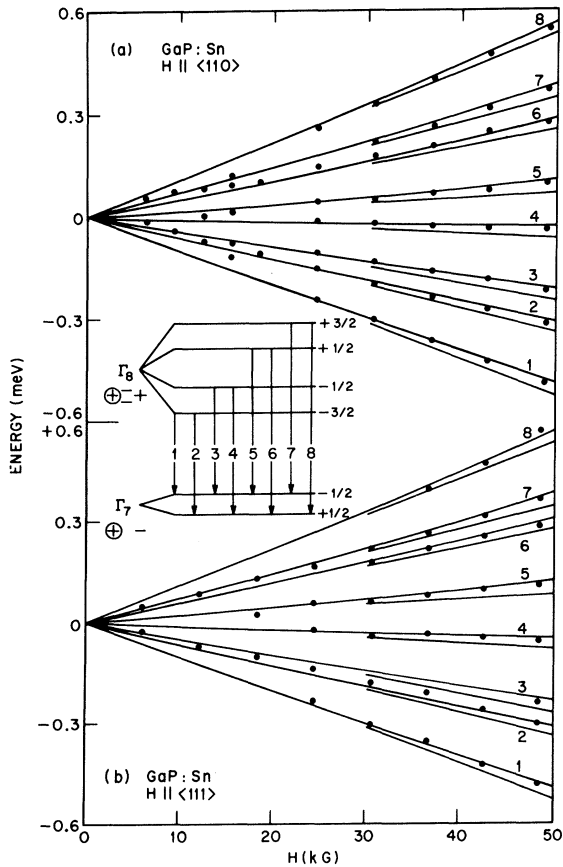
FIG. 9. Zeeman splittings of the Sn_1^0 line in GaP; (a) for $\vec{H} \parallel \langle 110\rangle$, and (b) $\vec{H} \parallel \langle 111\rangle$. Energies are measured relative to the zero-field Sn_1^0 line at 2.31786 eV. The lines are theory, the points experimental. The short straight lines drawn between 30 and 50 kG show the deviation from experiment for a linear Zeeman effect. The curved lines are calculated taking into account the magnetic interactions of the $\Gamma_7(p_{1/2})$ transition ground state with the nearby $\Gamma_8(p_{3/2})$ donor state assuming a separation of 2 meV (Fig. 6). The inset shows the magnetic splittings derived for the unpaired hole in the initial state and the single electron in the final state.
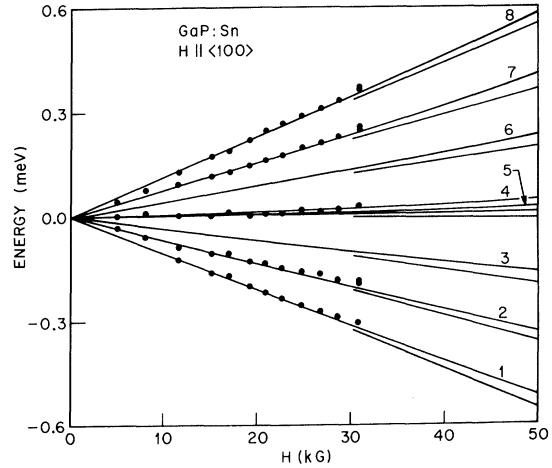
FIG. 10. Zeeman splittings of the Sn_1^0 line in GaP for $\vec{H} \parallel \langle 100\rangle$. The points are experimental and the solid lines theoretical, and energies are measured relative to the zero-field Sn_1^0 line as in Fig. 9. Components 3 and 6 ($\Delta m_j = 0$ transitions) are too weak to be measured in this orientation.

The final state has the magnetic splitting characteristic of the $J = \frac{1}{2}$ $p_{1/2}$ donor ground state

$$H_{fin} = -\frac{1}{3}g_e\mu_B\vec{J}\cdot\vec{H} \quad , \quad (8)$$

with the g factors

$$K = 0.67 \pm 0.02, \quad L = 0.17 \pm 0.02, \quad g_e = 1.95 \pm 0.06 \quad .$$

The assignment of the hole g factor to the initial state of this luminescence transition is derived
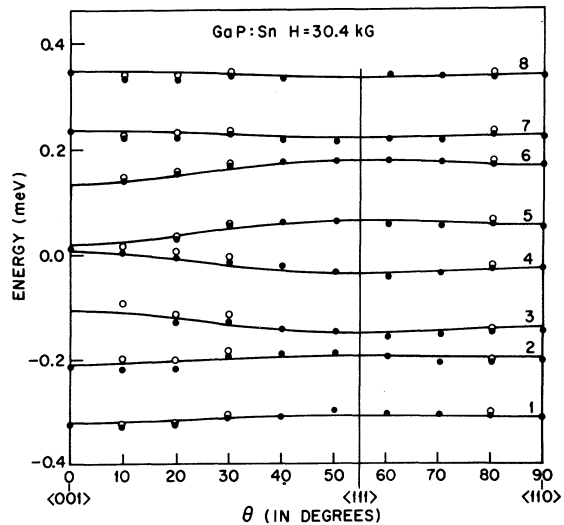
FIG. 11. Orientational dependence of the Zeeman splittings of the Sn_1^0 line in GaP at 30.4 kG. Points are experimental, solid lines are theoretical, taking account of the interaction between the Γ_7 and Γ_8 components of the donor ground state (Fig. 6). The open circles are experimental data measured outside the range of θ shown, and folded back about the $\langle 001\rangle$ and $\langle 110\rangle$ settings.

from the thermalization data in Fig. 12. Note particularly, that the intensity ratios of lines 1 and 2; 3 and 4; 5 and 6 do not change, whereas the intensity ratios 3/1; 5/1; 7/1 and 4/2; 6/2; 8/2 increase markedly with increase in excitation intensity (local lattice temperature) in a way qualitatively consistent with expectation from the magnetic substate diagram in Fig. 9. The sign of the electron g factor in the ground state of this transition is consistent with the polarization properties of the magnetic subcomponents (Fig. 13). For dipole transitions, only lines 3 and 6 should appear in $\vec{E} \parallel \vec{H}$, whereas all other lines are polarized $\vec{E} \perp \vec{H}$. If the effective g factor
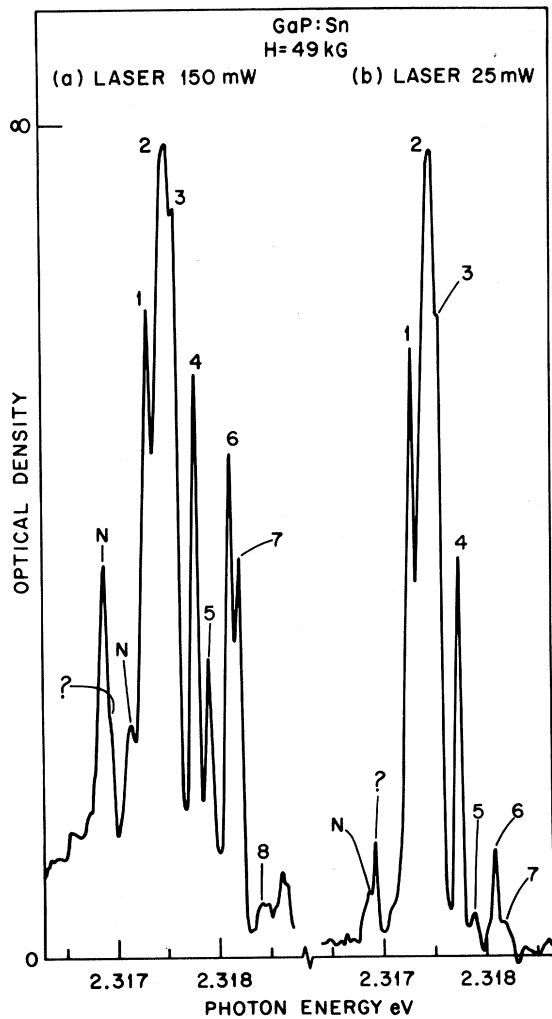

FIG. 12. Zeeman spectra of the Sn_1^0 line in GaP recorded photographically at 49 kG; (a) at high intensity of optical excitation by the sharply focused Ar^+ laser, and (b) at low excitation intensity (He-bath temperature 1.6 °K). Changes in relative intensity of the magnetic subcomponents due to thermalization in the Γ_8 excited state of the transition (Fig. 9) are clearly seen and are discussed in the text. The N-exciton no-phonon components are stronger in (a).
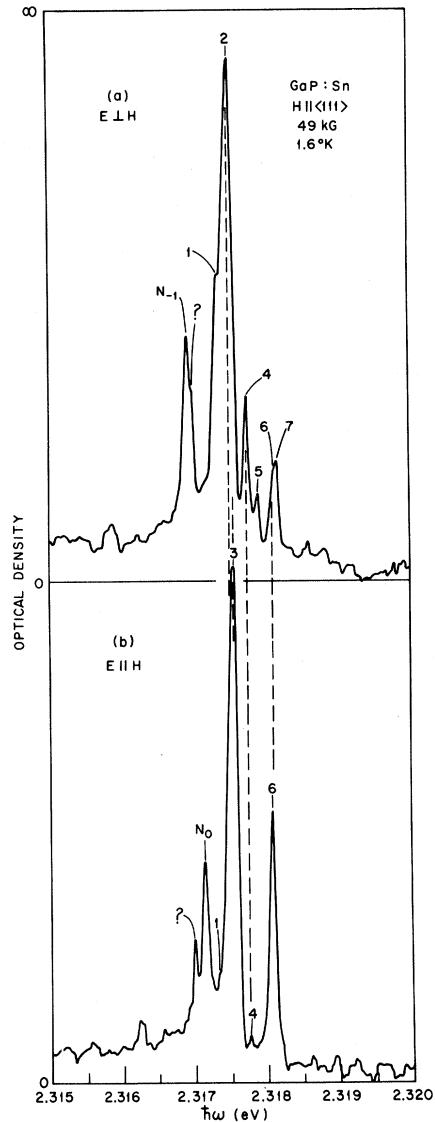

FIG. 13. Zeeman spectra of the Sn_1^0 line in GaP recorded photographically at 49 kG and a nominal (bath) temperature of 1.6 °K; (a) for σ components ($\vec{E} \perp \vec{H}$), and (b) for π components ($\vec{E} \parallel \vec{H}$). The polarization properties are discussed in the text. Note that the central component N_0 of the N "A line" is π polarized, whereas the outer components such as N_{-1} are σ polarized, as previously reported (Ref. 31 and 32).

of the Sn donor were positive, lines 4 and 5 would appear in $\vec{E} \parallel \vec{H}$. However, on this assignment lines 2 and 7 should be dipole forbidden. In fact, these lines are very strong (Figs. 12 and 13), line 2 being the strongest line in the spectrum. Much of its intensity is due to thermalization, but it is significant that line 2 is appreciably stronger than line 1. This difficulty remains unexplained. Quadrupole transitions would favor line 2 over the others, but the polarization data of Fig. 13 are inconsistent with qua-

drupole transitions.

It is necessary to include within the model inter- actions between the $p_{3/2}$ and $p_{1/2}$ donor states to ac- count for the nonlinear shifts of the levels at high magnetic fields. These shifts are shown explicitly in Figs. 9 and 10. Analysis of the data by Eq. (4) with $g_L = 0$ and $g_S = g_e = 1.95$ yields a value of the spin-orbit splitting $\Delta = 2^{+2}_{-1}$ meV, consistent with the value of 2.1 meV measured directly from the zero- field spectra (Sec. III B). This analysis of the Zee- man data shows that the ground state of the Sn do- nor is the $p_{1/2}$ state and that the initial state of the exciton bound to the neutral Sn donor (two electrons + one hole) has the two electrons paired off in the $p_{1/2}$ state, leaving only the weakly bound hole to contribute to the magnetic splittings in the Γ_8 initial state (Figs. 6 and 9).

We have seen that "two-electron" transitions are present in the zero-field spectra, in which the donor is left in a shallow (2.1-meV) excited state (Sec. III B). This excited state is assigned as the upper member of the pair of states derived from the p-like donor ground state by "spin-orbit" interaction (Fig. 6), the only energetically feasible possibility. Within the "sudden" approximation, in which one Γ_7 electron and the hole instantaneously disappear from the initial state, leaving a single electron in a Γ_7 state on the donor, the only final states which can be reached in the optical transition are those having Γ_7 symmetry. It is therefore not surprising that the transition to the $p_{3/2}$ (Γ_8) donor state is very weak compared to the principal transition. The intensity ratio $\mathrm{Sn}^0_{1,x}/\mathrm{Sn}^0_1$ is $\sim 7 \times 10^{-3}$, whereas the corresponding ratio $\mathrm{Sn}^{TA}_{1,x}/\mathrm{Sn}^{TA}_1$ is $\sim 8 \times 10^{-2}$, of the same order as the corresponding ratio for the LA and TO phonon-assisted components (Fig. 5). This suggests that the selection rule against these two- electron transitions from the Γ_8 initial state is relaxed through interaction with MC phonons from X.

There are spectral components which do therm- alize relative to Sn^0_1, in particular Sn^0_2 and Sn^0_3 shown in Figs. 4 and 5. These can be assigned to transitions from excited states of the bound-exciton complex to the $p_{1/2}$ ground state. As discussed in Sec. III B, there are replicas of each of these transitions, dis- placed 2.1 meV to lower energy, which are transi- tions from the excited initial states to the $p_{3/2}$ ground state (the $\mathrm{Sn}_{2,x}$ series in Fig. 5). The in- tensity ratio $\mathrm{Sn}^0_{2,x}/\mathrm{Sn}^0_2$ is ~ 0.5, nearly 100 times larger than $\mathrm{Sn}^0_{1,x}/\mathrm{Sn}^0_1$. This is understandable simply by noting that the lower excited states of the bound exciton must contain one electron in the Γ_7 state and the other in the Γ_8 state. The argument from the "sudden" approximation then fails to dis- criminate against transitions to either of the two components of the spin-orbit split ground state.

The level diagram in Fig. 6 summarizes the

knowledge gained from the luminescence spectrum. The ordering of the $p_{3/2}$ and $p_{1/2}$ Sn donor states is the same as for the spin-orbit split valence-band maximum in III-V compounds like GaP. Table III shows that the values of the g factors K, L, and g_e for the Sn exciton transitions are in close agree- ment with parameters for the P-site donor S in GaP. The hole g factor is much more nearly iso- tropic for excitons bound to the Ga-site acceptor Cd and to the P-site isoelectronic trap N.

D. Electronic Structure of the Bound Exciton: Piezospectroscopic Effects

The splitting of the N and S bound excitons shown in Fig. 14 is due to the strain splitting of the va- lence band, since electrons bound to these impuri- ties are in the $1s(A_1)$ valley-orbit state[31,32] which does not split under stress.[33] Balslev[33] has ob- served a nearly isotropic splitting of a near-gap bound exciton in GaP, which he identified with S but we believe is due to N. The splitting coefficient (dE/dF) for N in Fig. 14(a) ($\vec{F} \parallel \langle 111 \rangle$) is 0.61 meV kg^{-1} mm^2, or about 1.7 times greater than reported by Balslev and confirmed by Dean and Faulkner.[34] We believe that this discrepancy is caused by sam- ple bowing, so that the effective stress in the ~ 65-μ surface layer in which the luminescence is created is appreciably larger than the average stress. The previous measurements of this coefficient[33,34] were made in absorption, which samples the whole cross section of the crystal so that the effects of stress inhomogeneity are more evident in the raw data.

The coefficient dE/dF for the N exciton is $\sim 25\%$ smaller than S [Fig. 14(a), $\vec{F} \parallel \langle 111 \rangle$], indicating that the hole deformation potential is sensitive to the center to which the exciton is bound. Piezo- spectroscopic studies of the intrinsic interband absorption[33,34] indicate that the intrinsic exciton splits like the N bound exciton rather than S. The coefficient $(dE/dF)_S$ for $\vec{F} \parallel \langle 110 \rangle$ from Fig. 14(b) is $\sim 10\%$ larger than for $\vec{F} \parallel \langle 111 \rangle$ [Fig. 14(a)]. This difference may not be significant in view of the in- homogeneity in the stress applied to these crystals.

We are more concerned with the comparative behavior of the Sn and S excitons in Fig. 14 than with the absolute splitting rates. Transitions Sn^0_1 and S^0 both split into just two components for $\vec{F} \parallel \langle 111 \rangle$, with identical coefficients (dE/dF) [Fig. 14(a)]. The upper component thermalizes into the

TABLE III. g factors derived from magneto- optical studies of shallow bound excitons in GaP.

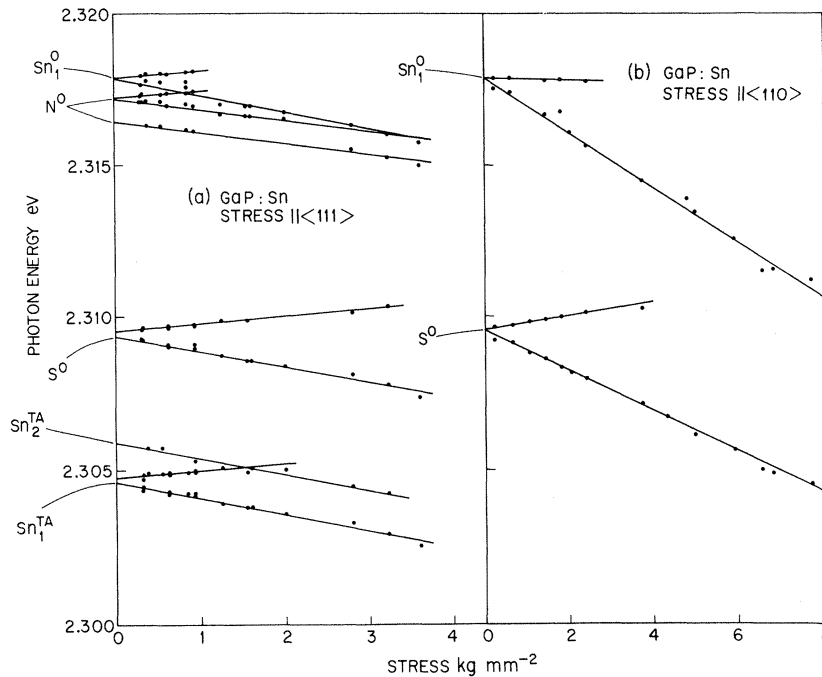| g factor	Sn(Ga site)	S(P site) (Ref. 31)	Cd(Ga site) (Ref. 18)	N(P site) (Ref. 32)
K	0.67 ± 0.02	0.65 ± 0.07	0.94 ± 0.04	0.95 ± 0.04
L	0.17 ± 0.02	0.15 ± 0.05	-0.07 ± 0.03	0.03 ± 0.02
g_e	1.95 ± 0.06	1.89 ± 0.06	$\cdots$	1.96 ± 0.03

FIG. 14 Splittings of some no-phonon (Sn_1^0, N^0, S^0) and phonon-assisted ($Sn_{1,2}^{TA}$) lines for excitons bound to neutral Sn and S donors and to the N isoelectronic trap in GaP recorded at ~ 5 °K under uniaxial stress; (a) $\parallel \langle 111 \rangle$, and (b) $\parallel \langle 110 \rangle$. The splitting rates of the Sn and S lines are identical within experimental error in all cases, while that of the N^0 line shown only for stress $\parallel \langle 111 \rangle$ is ~ 25% less. The intensities of the upper subcomponents of each line decrease rapidly with increasing stress, indicating that all splittings are in the excited state and are due to the hole (see text). Note particularly, that the center of gravity of all these split lines vary identically for stress $\parallel \langle 111 \rangle$, but are very different for the S and Sn excitons for stress $\parallel \langle 110 \rangle$ (see text).

lower indicating that the splitting is in the excited state of the transition. There is no evidence of a ground-state splitting. No splitting of conduction-band states is expected, since $\langle 111 \rangle$ stress affects all $\langle 100 \rangle$ minima equally. The observed splitting is due to the hole derived from the Γ_8 valence-band maximum. The upper component is polarized $\vec{E} \perp \vec{F}$ ($\vec{E}$ is the electric vector), while the lower appears in $\vec{E} \parallel \vec{F}$ for Sn_1^0, N^0, and S^0. This confirms that the $m_J = \pm \frac{1}{2}$ component of the stress-split $J = \frac{3}{2}$ valence-band maximum moves towards the conduction band for compressive stress in GaP.[33]

Figure 14(b) shows that Sn_1^0 also splits into just two components for $\vec{F} \parallel \langle 110 \rangle$. This confirms the energy-level scheme in Fig. 6, since a significant stress-induced splitting is expected for the Γ_8 state of the Sn donor. The components of this extra splitting would not show thermalization, and would be clearly seen if the Sn_1^0 transition terminated on the Γ_8 donor state. We are unable to confirm this predicted splitting of the Γ_8 state, since the Sn_{1x} "two-electron" transitions were indistinct in the stress spectra. For similar reasons, it was difficult to establish the splitting patterns of the $Sn_{2,3}^0$ excited states.

An interesting difference between the behavior of the Sn_1^0 and S^0 transitions is apparent in Fig. 14(b). We find that the (negative) coefficient (dE/dF) for center of gravity (cg) of the Sn_1^0 transition is much larger than for S^0 and N^0, which show similar cg shifts about 25% lower than reported by Balslev.[33] This difference originates in the anisotropic strain

splitting of the three-valley conduction band of GaP.[33] The effect of the anisotropy is negligible for an electron in the singlet $1s(A_1)$ state, entering only in the small nonlinear shift of this state, if the valley-orbit splitting $1s(E) - 1s(A_1) \gg$ the stress-induced splitting of the $1s(E)$ state. This approximation is appropriate for the S and N excitons. However, we have seen that the spin-orbit splitting of the Sn exciton is rather small compared with the stress splittings in Fig. 14. Since the donor states cannot split for $\vec{F} \parallel \langle 111 \rangle$, we can take the differential shift of the cg of Sn_1^0 between $\vec{F} \parallel \langle 110 \rangle$ and $\vec{F} \parallel \langle 111 \rangle$ as a measure of the valley strain splitting for the former direction. For $\vec{F} \parallel \langle 110 \rangle$, the lowest-energy electron state shifts according to[29]

$$\frac{dE}{dF} = -\frac{1}{3}(S_{11} - S_{12}) \times \frac{2}{3} \Xi_u \ . \tag{9}$$

This contribution will cause the lower component of the Sn_1^0 transition to shift down faster than that of the S exciton, the shift of the latter being almost entirely due to the stress splitting of the $p_{3/2}$ valence-band maximum. According to the values of the compliance constants S_{11}, S_{12} and the deformation potential Ξ_u determined by Onton and Taylor,[29] Eq. (9) predicts an excess downward shift of 1.5 meV at $F = 8$ kg mm^{-2} for the lower component of Sn_1^0 compared with S^0. The experimental value is 1.9 meV according to Fig. 14(b). In view of the scatter in the data in Fig. 14(b) and the underestimate of the stress scale discussed above, the agreement between experiment and theory is reasonable. The data is insufficiently precise to define the non-

linear effects expected at low stress due to the stress-induced interactions of the Γ_7 and Γ_8 donor states.

The predicted contribution of the conduction-band splitting to the downward shift rate of the lower component of Sn_1^0 at high $\langle 100 \rangle$ stress is four times that in Eq. (9). We have observed an excess shift of Sn_1^{TA} compared with S^0 of ~ 9 meV at $F = 8$ kg mm^{-2} $\| \langle 100 \rangle$, in fair agreement with this prediction. Again, no ground-state splitting was seen for the Sn_1 transition.

E. Absorption and Recombination Lifetime of Excitons Bound to Neutral Tin Donors

The extrinsic features in the absorption edge spectrum of the heavily Sn-doped crystal shown in Fig. 15 are dominated by the sharp line N^0 due to the photocreation of excitons bound to N isoelectronic traps. However, the strength of this line indicates only ~ 1.5×10^{16}-cm^{-3} optically active nitrogen. The S^0 bound exciton line, indicating the presence of ~ 3×10^{15}-cm^{-3} neutral S donors, is just visible. In addition, weak absorption containing some structure appears between the exciton energy gap E_{gx} and $E_{gx} + \hbar \omega_{TA}$, the threshold energy for intrinsic absorption.[35] Much of this extrinsic absorption is contained in the broad line at 2.3285 eV and the associated plateau at higher energies, which is a persistent unidentified feature of GaP crystals grown by the liquid encapsulated Czochralski method.

In addition, there are two pairs of weak absorption lines near 2.332 and 2.350 eV. The lower-energy members of each pair lie, respectively, 13.1 and 31.5 meV above component Sn_1^0 (Fig. 4), and are therefore believed to represent the photocreation of the Sn_1^0 bound-exciton state with the emission of TA and LA MC phonons (Table I). The broad higher-energy components Sn_α^{TA} and Sn_α^{LA} are believed to represent MC TA and LA phonon-assisted absorption processes in which higher-energy states of the Sn exciton are created. The no-phonon component associated with these latter bands should occur at ~ 2.320 eV. Since the components Sn_α^{TA}, Sn_α^{LA}, Sn_A^{TO} in Fig. 4 also indicate a no-phonon component near 2.320 eV, we label these MC phonon-assisted absorption components accordingly. It is evident from Fig. 15 that the strength of the ~ 2.320-eV no-phonon component is much less than its MC phonon replicas. The low no-phonon intensity of higher excited states of the Sn exciton is consistent with the trend of the oscillator strength ratios $Sn_2^0/Sn_1^0 = 0.57$ and $Sn_3^0/Sn_1^0 = 0.27$ estimated from the luminescence spectrum at 4.2 °K, assuming thermal equilibrium between these excited states, and also with the absence of component Sn_α^0 in Fig. 4.
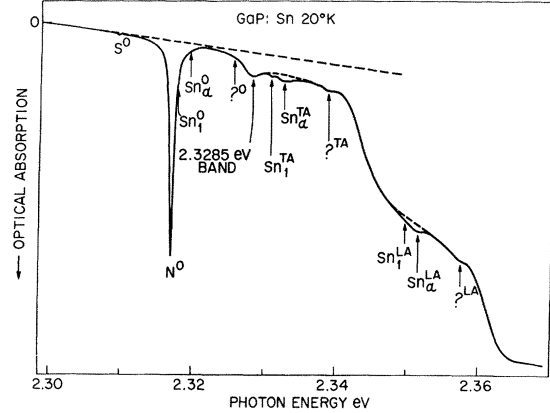
The intensity ratio of absorption components

FIG. 15. Low-temperature near-gap absorption of GaP containing ~ 5×10^{17}-cm^{-3} neutral Sn donors, showing the weak absorption due to Sn, as well as absorption due to residual N and S. The series $?^{0, TA, LA}$ do not involve the same transition as in Fig. 4.

Sn_1^{LA}/Sn_1^{TA} is ~ 3 according to Fig. 15, consistent with the more accurate value obtained from the luminescence spectrum (2.6 according to Table II). Using the intensity ratios in the luminescence spectrum, and the observed strength of absorption component Sn_1^{TA}, we can therefore calculate the total absorption strength of the Sn exciton transition. Hall-effect measurements on the crystal used for Fig. 15 indicated that $N_D - N_A = 5.3 \times 10^{17}$ cm^{-3}, with $E_D = 56$ meV (Sec. III A). From these quantities, the total oscillator strength f of the Sn_1 exciton transition can be estimated with the relation

$$(N_D - N_A)f = 9.6 \times 10^{12} n(\alpha \Gamma) \ , \tag{10}$$

appropriate for Gaussian-broadened transitions at shallow impurity states in a semiconductor. Here, n is the refractive index (3.47 near Sn_1^0) and $(\alpha \Gamma)$ is the total absorption area in cm^{-1} meV. Using Eq. (10), the absorption of Sn_1 in Fig. 15 indicates that $f \sim 10^{-5}$. This is slightly smaller than expected from the f values of the P-site donors, derived by assuming the f values of the MC phonon-assisted replicas to be invariant for different donor-exciton complexes.

The radiative decay time τ_r corresponding to $f = 10^{-5}$ for the Sn_1 transition is 250 μsec according to the relationship

$$\tau_{rad}^{-1} = (nf/1.5\lambda^2)g_1/g_2 \ , \tag{11}$$

where λ is the wavelength of the Sn exciton and g_1 and g_2 are the degeneracies of the ground and excited states of the transition (respectively, 2 and 4 according to Sec. III C).

Experimentally, the characteristic time τ_e of the exponentially decaying Sn_1 luminescence is only 90 nsec (Fig. 16). By analogy with S donor exciton complexes in GaP,[6] we presume that the large ratio
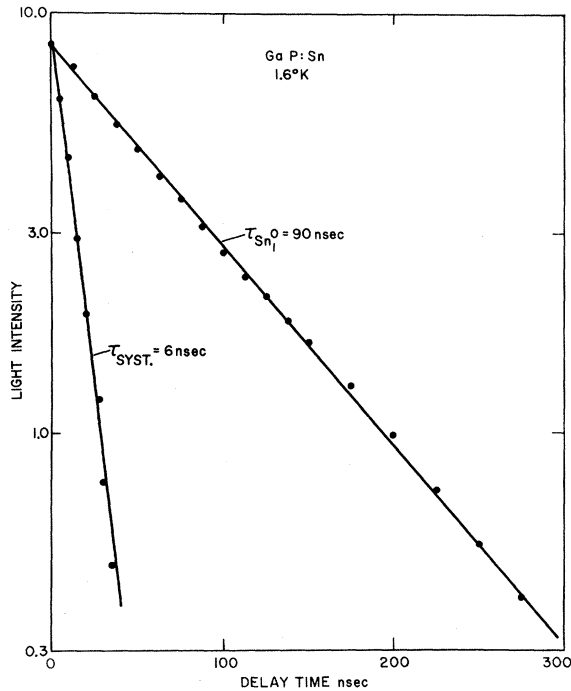
FIG. 16. Time decay of light in the Sn_1^0 luminescence line in GaP compared with the response of the detecting system to the light from the acousto-optically modulated Ar^+ laser used to excite the luminescence. The decay of the luminescence is exponential over the indicated dynamic range provided by the sampling scope display. The intensity of the fast decaying exciting light decreases faster than exponentially, but has the "average" time constant shown.

τ_r/τ_e indicates that this bound exciton decays predominantly by a nonradiative process, and nominate the Auger effect. Similar behavior has been observed recently in the decay of excitons at neutral acceptors in GaP,[18] where again there is a third electronic particle (here a hole) to carry off the energy of the transition as kinetic energy.

IV. SUMMARY

We have shown that an accurate value of the ionization energy of the donor Sn, 65.5 ± 1 meV, may be derived from high-resolution measurements of donor-acceptor-pair luminescence spectra at low temperatures, as has been done for many other donors and acceptors in GaP. This is possible even though the Ga-site donor Sn induces only very weak no-phonon pair transitions because of the symmetry properties of electrons bound to such donors. We have also shown that reasonable estimates of $(E_D)_{Sn}$ may be obtained from an intercomparison of the energies of narrow distant pair spectrum peaks recorded at very low levels of excitation for suitably chosen pairs of donors and acceptors. Tin is by far the shallowest donor identified so far in GaP,

although its ionization energy is ~ 25 meV larger than theoretical estimates of the effective-mass ionization energy of donors in GaP.[9]

A bound-exciton spectrum characteristic of GaP:Sn has been identified with the luminescence of excitons bound to neutral Sn donors with a localization energy of ~ 10 meV.[36] Magneto-optical studies confirm this model and indicate that in the ground state of the principal exciton transition the Sn donor electron is in a $p_{1/2}$ state with a g factor of $-\frac{1}{3} g_e$, as predicted by theory. Analysis of nonlinear shifts in the Zeeman spectra and direct observation of "two-electron" transitions in the zero-field spectra show that the $p_{3/2}$ donor state lies close to 2 meV above the $p_{1/2}$ state. This splitting is due to spin-orbit interaction, the electron on the Ga-site donor Sn being p-like because of contributions from the three equivalent $\langle 100 \rangle$-type conduction-band valleys in GaP. This is the first detailed experimental investigation of the symmetry properties of such a donor. Piezospectroscopic studies show that the donor ground state does not split under uniaxial stress directed along $\langle 100 \rangle$, $\langle 110 \rangle$, or $\langle 111 \rangle$ crystallographic axes, supporting the assignment as a $p_{1/2}$ state. We were not able to test the assignment of the ~ 2-meV donor excited state as $p_{3/2}$ because the "two-electron" transitions through which it is seen are too weak for detailed study under uniaxial stress. However, anisotropic shifts observed in the lowest component of the Sn_1 transition were consistent with the stress-induced interaction expected at high stress for the $p_{1/2}$ and $p_{3/2}$ donor states. The lifetime of the Sn exciton luminescence is 90 nsec, 2700 times shorter than the prediction from the absorption strength of this transition according to detailed balance. As has been done for other donor- and acceptor-exciton complexes in GaP, we interpret this enormous ratio as evidence that the decay of the Sn exciton is dominated by a nonradiative Auger channel. This assumption is qualitatively consistent with the low efficiency of the Sn exciton luminescence, even at low temperatures in crystals where the Sn exciton dominates the near-gap luminescence (Fig. 4).

Note added in proof. Magnetic contributions due to the orbital part of the wave function of electrons bound to the Sn donor in GaP have been observed recently in electron-spin resonance studies.[37] Typical g factors for this contribution are within the error limits for Ge given in Table III. This effect is therefore too small to be seen readily in optical Zeeman studies.

---

*Present address: National institute for Researches in Inorganic Materials, Tokyo, Japan.

[1]D. G. Thomas, M. Gershenzon, and J. J. Hopfield, Phys. Rev. 131, 2397 (1963).

[2]P. J. Dean, Phys. Rev. 157, 655 (1967).

[3]T. N. Morgan, Phys. Rev. Letters 21, 819 (1968).

[4]P. J. Dean, C. J. Frosch, and C. H. Henry, J. Appl. Phys. 39, 5631 (1968).

[5]T. N. Morgan, T. S. Plaskett, and G. D. Pettit, Phys. Rev. 180, 845 (1969).

[6]D. F. Nelson, J. D. Cuthbert, P. J. Dean, and D. G. Thomas, Phys. Rev. Letters 17, 1262 (1966).

[7]H. W. Verleur and C. M. Ringel, Proceedings of the 137th National Meeting of the Electrochemical Society, 1970, Abstract Nos. 68 and 190 (unpublished.

[8]D. Maydan, IEEE J. Quant. Electron. QE-6, 15 (1970).

[9]A. Onton, Phys. Rev. 186, 786 (1969).

[10]F. A. Trumbore and D. G. Thomas, Phys. Rev. 137, A1030 (1965).

[11]Lyle Patrick and P. J. Dean, Phys. Rev. 188, 1254 (1969).

[12]The radii of holes bound to neutral Zn acceptors and electrons bound to neutral Sn donors are very similar, ~ 13 Å.

[13]L. I. Schiff, *Quantum Mechanics* (McGraw-Hill, New York, 1955), pp. 176—180.

[14]P. J. Dean, E. G. Schönherr, and R. B. Zetterstrom, J. Appl. Phys. 41, 3474 (1970).

[15]H. C. Montgomery (private communication).

[16]H. C. Montgomery and W. L. Feldman, J. Appl. Phys. 36, 3228 (1965).

[17]H. C. Casey, Jr., F. Ermanis, and K. B. Wolfstirn, J. Appl. Phys. 40, 2945 (1969).

[18]P. J. Dean, R. A. Faulkner, and S. Kimura, Solid State Commun. 8, 929 (1970).

[19]The no-phonon line for an exciton bound to the ionized Sn donor must lie at least $(E_D)_{Sn}$ below E_g, i.e., at least 45 meV *below* the lowest-energy component Sn_1^0. This type of transition is not observed for donors in GaP.

[20]J. L. Yarnell, J. L. Warren, R. G. Wenzel, and P. J. Dean, *Neutron Inelastic Scattering* (International Atomic Energy Agency, Vienna, 1968), Vol. I, p. 301.

[21]P. J. Dean, Luminescence 1, 2 398 (1970).

[22]F. J. Morin, T. H. Geballe, and C. Herring, Phys. Rev. 105, 525 (1957).

[23]D. S. Nedzvetskii, B. V. Novikov, N. K. Prokof'eva, and M. B. Reifman, Fiz. Tekhn. Poluprov. 2, 1089 (1968) [Soviet Phys. Semiconductors 2, 914 (1969)].

[24]The binding energy of the $2p$ state of the Si donor is 7.3 meV according to Ref. 9. The Sn donor should exhibit a very similar value. The binding energy of the s-like envelope excited states of the Sn donor can be estimated from the $1s$ state using the quantum-defect method. Taking $E_{1s} = 64$ meV as the weighted average of the $p_{1/2}$ and $p_{3/2}$ components, we find $E_{2s} = 12.2$ meV and $E_{3s} = 5.0$ meV. The spin-orbit splittings of these excited states calculated from the 2.1-meV ground-state splitting are negligible. The former is in very good agreement with the binding energy derived from the 53.2-meV

"two-electron" transition energy, but the latter is in poor agreement with the value from the 58.5-meV component. In view of this and the relative intensities of components Sn_1^x in Fig. 4, it is likely that the 53.2-meV component represents two-electron transitions to the $2s$ excited state, and the 58.5-meV component represents transitions to the $2p$ excited state, transitions to higher s- and p-like excited states being too weak to appear against the multiphonon sidebands. The "two-electron" spectra of P-site donors in GaP contain only transitions to s-like excited states (Refs. 9 and 29) in which the $1s(A_1) \rightarrow 2s(E)$ transition predominates.

[25]P. J. Dean, J. D. Cuthbert, D. G. Thomas, and R. T. Lynch, Phys. Rev. Letters 18, 122 (1967).

[26]"Two-hole" replicas of the weak no-phonon transitions in the neutral-acceptor bound-exciton spectra in GaP were observed only weakly for the deep acceptor Cd.

[27]In the limit that the approximation to the bound-exciton wave function shown in Fig. 7(a) becomes rigorous, the bound-exciton state disappears.

[28]J. R. Haynes, Phys. Rev. Letters 4, 361 (1961).

[29]A. Onton and R. C. Taylor, Phys. Rev. B 1, 2587 (1970).

[30]Strictly speaking, the g factor would be very small compared to 2. It would be nonzero only because of a small penetration of the central core of the impurity by the donor envelope wave function.

[31]Y. Yafet and D. G. Thomas, Phys. Rev. 131, 2405 (1963).

[32]J. L. Merz, R. A. Faulkner, and P. J. Dean, Phys. Rev. 188, 1228 (1969).

[33]I. Balslev, J. Phys. Soc. Japan Suppl. 21, 101 (1966).

[34]P. J. Dean and R. A. Faulkner, Luminescence 1, 2, 552 (1970).

[35]P. J. Dean and D. G. Thomas, Phys. Rev. 150, 690 (1966).

[36]This is the first such Ga-site donor-exciton complex so far identified in GaP. A bound exciton with a localization energy of ~ 14 meV is a persistent feature of Si-doped GaP. This value of E_{BX} is consistent both with the decay of an exciton bound to the neutral Si acceptor [consider Fig. 3 in Ref. 18, with $(E_A)_{Si} = 203$ meV] as suggested in Ref. 20 (Fig. 4 caption), and with the decay of an exciton bound to the neutral Si donor [consider Fig. 8 of this paper, with $(E_D)_{Si} = 82$ meV]. The 0.52-meV splitting in the ground state of this transition ($P_0^1 \rightarrow P_0$ in Fig. 4 of Ref. 20, also Ref. 21) might be attributed to the $\Gamma_7 \rightarrow \Gamma_8$ spin-orbit splitting of the Si donor on the latter identification, but it is not yet clear whether the magneto-optics of this transition are consistent with this assignment. It is more difficult to study the behavior of the Si exciton, since Si enters the GaP lattice on both sites. Most of the recombinations occur through Si donor-acceptor pairs at moderate Si concentration, because the excitation tunnels to these deeper states from the shallow bound excitons such as P_0.

[37]F. Mehran, T. N. Morgan, and R. S. Titte (unpublished).